Journal of Thermal Analysis and Calorimetry
https://doi.org/10.1007/s10973-019-08166-z

Calorimetry and thermal analysis in food science: an updated review

Alberto Schiraldi[1,2] · Dimitrios Fessas[1,2]

Received: 27 October 2018 / Accepted: 28 February 2019

Abstract

Food science is a domain of life science. Applications of thermal analysis and calorimetry (TAC) to food products deal with many investigation targets spanning from the characterization of the systems at molecular and supramolecular level to the description of the microbial metabolism. Food products are multi-phase and multi-component metastable systems where several processes can occur simultaneously during the preparation process and the shelf life. One therefore has to disentangle various contributions to the overall instrumental outputs, using appropriate data treatments and kinetic models, and/or results from other experimental approaches. The paper reports an updated survey of TAC applications to food products through specific examples of data treatments.

Introduction

The first European paper devoted to thermal analysis and calorimetry (TAC) applied to food products and processes appeared in 1990 [1], followed by wider presentations in 1994 [2] and 1999 [3]. In that decade, food science actually became a special domain of TAC application to life science (Scheme 1), including many appealing subjects as investigation targets, since food products are multi-component and multi-phase metastable systems that host living microbial cells.

As for the molecular and, above all, supramolecular aspects, food science actually is a branch of polymer science [4] in as much as natural polymers govern the overall behavior of most food products. Food polymers are indeed responsible for phase separations [5], which determine the extension of the interphase regions where most of the chemical reactions take place. Food polymers directly affect the overall viscosity of the system and consequently the diffusion rate of reactants with the ultimate limit of the glass transition, below which no molecular displacement can occur. This threshold mainly depends on the local polymer concentration, which is not necessarily uniform across the system because of: (a) the thermodynamic incompatibility that induces phase separation and (b) the large viscosity related to the presence of the polymers themselves. Beside their viscosity effects, many food polymers act as surfactants (proteins, nonionic polyglycerides, propylene glycol alginate, etc.) that stabilize the dispersion of various phases within a given food system [6], allowing the persistence of bubbles, droplets, solid particles. (A good example is the ice cream.)

The other major component of most food systems is water. Its displacements and partition between coexisting phases (including dispersed phases) substantially contribute to the physical and sensory peculiarity of a given product [7]. Water enters the structure of biopolymers (carbohydrates, globular proteins and gluten) [8–12], since water molecules form bridges between polymer chains through hydrogen bonds [11]. In spite of its large mobility, water can remain trapped within a polymer network loosing many properties of bulk water, like the ability to form ice crystals or a vapor phase at the temperature where one would expect it to do so. The "bound" water is indeed a very popular parameter of food science as it determines the practice of industrial preparations, like frozen dough for bakery, ice cream, jellies, etc., and of some processes like lyophilization [13], thermal [14] and osmo-dehydration [15]. These aspects actually are consequences of the role of water on the glass transition temperature, T_g, of wettable, or water-trapping products, including powdered materials (sugars, coffee, cocoa, etc.) [4, 16, 17].

Because of such interactions, polymers and water make the preparation of food a true endeavor, especially at the industrial scale. Once the various ingredients and

✉ Alberto Schiraldi
alberto.schiraldi@unimi.it

[1] Department of Chemistry, University of Milan, Milan, Italy

[2] Department of Food Environmental Nutrition Sciences, University of Milan, Milan, Italy

Journal : Large 10973 | Dispatch : 4-3-2019 | Pages : 12
Article No. : 8166 | ☐ LE | ☐ TYPESET
MS Code : JTAC-D-18-02033 | ☑ CP | ☑ DISK

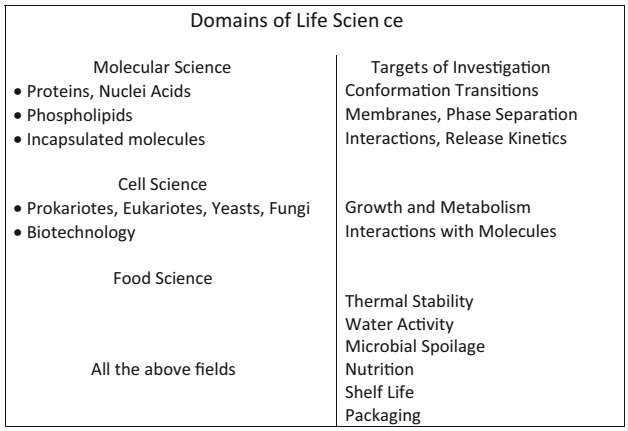

Scheme 1 Domains of life science to investigate with TA and calorimetry

respective doses are established, the preparation requires an adequate procedure to account for the phase dispersion and the overall viscosity at each step of the process. This picture is even more complex because of the concomitant presence of microbes that are responsible for many chemical and physical changes that affect sensory and nutritional properties of most food products. At the household scale, the heritage of previous experiences, namely the culinary traditions, unconsciously complies with these physical and microbiological constraints, although, nowadays, a better awareness of the physics involved is at the fundament of the so-called molecular gastronomy [18] that suggests novel approaches to food preparation. Unfortunately, this is not enough for processes at the industrial scale.

The whole panoply of TAC (IC, DSC, TMDSC, TG, DMA, etc.) allows a thorough inspection of food systems through the quantitative determination of many properties and processes, like enthalpy and heat capacity changes, glass transition, phase separations, water activity and microbial growth [3]. The results of such investigations make the predictions of the shelf life reliable and provide a rationale for the production at the industrial scale. One just needs a representative sample of the system to investigate. According to the size of such sample, one has to select the kind of instrument to use. No pretreatment is normally required. Salads, cheese, milk, rice, chocolate, etc., can directly undergo the investigation. This possibility is of crucial importance as long as almost any food would lose its own physical and chemical properties once treated: Separation, extraction, filtration, etc., can substantially modify the food system.

Other techniques, like microscopy (including laser confocal microscopy), SEM, NMR, rheology, X-ray diffraction, etc., add the complementary information that supports the interpretation of the evidences garnered through calorimetry and thermal analysis.

The large number of experimental approaches nonetheless leaves unresolved the true challenge for food scientists: the simultaneous occurrence of many processes that take place in the course of the investigation of a given product. The direct output of a measurement can indeed be the resultant of many coexisting phenomena and therefore require a further treatment to split them from one another. Such a treatment can be mathematical (deconvolution of traces, kinetic models, etc.) and/or implies separate experiments on model systems.

In the present review, some examples allow one to envisage how a food scientist can convey the interpretation of the experimental TAC data into the familiar view of chemical thermodynamics and kinetics, or traditional microbiology, selecting parameters that are useful tools for an objective description of a given food product or process.

Bread and starchy products

Bread and dough

Bread, one the most diffused food, is the result of baking a dough formed by mixing cereal flours containing gluten with water, salt and yeast, or chemical leaven. In spite of the macroscopic appearance, the starting kneaded dough is, at room temperature, a rather heterogeneous system [19]. It contains starch granules (the size of which ranges from 5 to 50 μm), damaged starch granules, aqueous globular proteins and salts, dispersed non-starch polysaccharides (like arabino-xylans), partially linked glutenin and gliadin (precursors of the gluten), separated lipid fractions, yeast cells, etc. This system undergoes a substantial transformation when heated during the baking treatment. The formation of the gluten network takes place just after the onset of the starch gelatinization that encompasses a wide temperature range above 50 °C; the former process is exothermic, while the latter is endothermic. In the same temperature range, the globular proteins of the flour undergo unfolding (endothermic) and aggregation (exothermic). All these changes depend on the water content, occurring at higher temperature for lower humidity [20].

To complete the picture, one should account for the fact that the dough polymers (starch and non-starch carbohydrates, gluten and globular proteins) compete with one another for the solvation water and are thermodynamically incompatible with one another [21], which means that they tend to form separated aqueous phases dispersed within one another. The mean size of the dispersed particles (droplets, bubbles) ranges around 5 microns, while the gluten

Journal : Large 10973 Dispatch : 4-3-2019 Pages : 12
Article No. : 8166 LE TYPESET
MS Code : JTAC-D-18-02033 CP DISK

networks is a long-range extended structure that interpenetrates the amylopectin and amylose gels. What's more, because of the size of the loaf and the standard baking conditions, a large temperature gradient exists between the surface of the system, where T can attain 200 °C, and its core, where the T raises more slowly and remains below 100 °C (Fig. 1). This is the reason for a core-to-surface water migration [22]: Accordingly, the water content is not homogeneous across the system.

In a typical baking process, water escapes from the dough loaf and its final content is about half of the starting one. The main consequence is an overall hardening of the system, which, however, is not uniform at all. At its surface appears the crust (that implies local pyrolysis and oxidation because of the atmospheric oxygen), while its core becomes a sponge with irregular alveoli, namely the crumb. The formation of alveoli starts from original nuclei of gas phase (mainly CO_2 and water vapor produced by the added leaven) and continues during the baking progress with complete replacement of CO_2 with air [23]. The hardening of the walls that governs the average alveolar size is the resultant of the competition for the available moisture between the thermodynamic incompatible polymers mentioned above [24], among which globular proteins act as surfactants at the gas/liquid interface of the bubbles.

Now let us consider what happens in a DSC investigation of a dough sample that normally does not exceed 10 mg. Since the DSC cell is sealed, no water loss takes place. The temperature gradient across such a sample is much smaller than in a real dough loaf that undergoes baking. There is no formation of an external crust and an internal true crumb. One therefore may reasonably raise the question: Can a single DSC investigation shed some light on the changes that take place in a real baking process? The obvious the answer is "no".

To overcome the substantial differences between a DSC experiment and a real baking test, one has to perfect the information through other investigations, like DSC and TG runs performed with open cells [25], including Knudsen cells [26], and rheological tests [27]. However, in such conditions the large exothermal effect related to the water evaporation overwhelms any other heat exchange just in the temperature range where most of the interesting transformations take place. One cannot therefore rely on the overall thermal effect, but shall first take into account mass loss and temperatures of the main signals. Knudsen isothermal TG allows the estimation of the relative humidity (RH) of starting and final products [28]. Such multifacet approach allows one to recognize that starch gelatinization is not complete in most regions of the bread loaf, above all the crust, where the quick drying makes the water content insufficient to sustain the process [26]. This picture comes from DSC and TG investigations that allow definition of a TTT (time, temperature, transformation) diagram related to the starch gelatinization in a dough that undergoes baking [25].

The TTT diagram (Fig. 2) can be determined with several DSC investigations, each at a given heating rate. From every single DSC run, one can draw the corresponding trend of the gelatinization degree, $\alpha[T(t)]$, sweeping the area beneath the DSC signal [25]. One has, however, to take into account the simultaneous loss of moisture, which can be assessed with parallel TG investigations [25].

The RH is about 98% in the starting dough, but it drops below 80% in the crust and levels at about 95% in the crumb [28]. The gluten meshwork traps almost 15% of the moisture content of the crumb, while the rest of the moisture content, shared by starch and non-starch polysaccharides and globular proteins, undergoes easier displacements [29]. According to TG investigations, a starchy gel releases its moisture content continuously, producing a single DTG peak, while a gluten/water aggregate shows a double peak [29], which indicates the

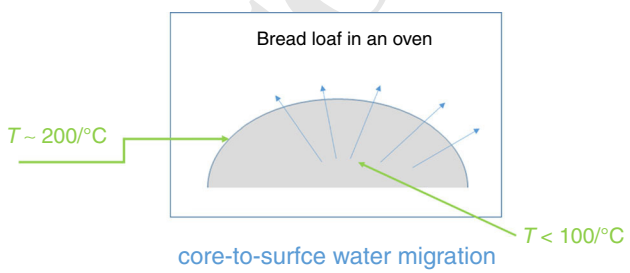

Fig. 1 Water displacement within a bread loaf undergoing baking in an oven

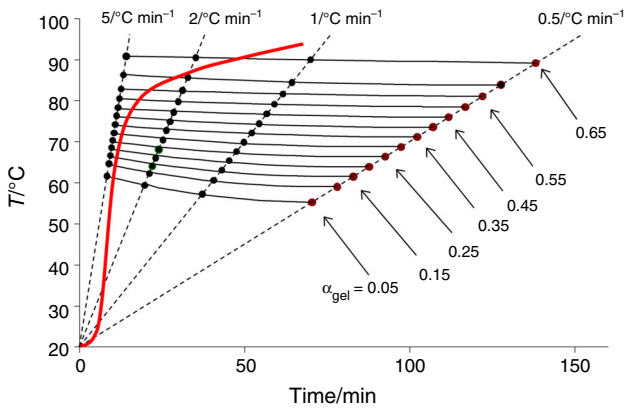

Fig. 2 TTT diagram related to the progress of starch gelatinization, $\alpha = \alpha(T)$, within a bread loaf undergoing baking. The red line reflects the actual thermal history at the loaf core. The straight dotted lines correspond to the DSC traces recorded at different heating rates (0.5, 1, 2 and 5 °C min^{-1}) while full tie lines are drawn across iso-α steps. Data from ref [25]

Journal : Large 10973 | Dispatch : 4-3-2019 | Pages : 12
Article No. : 8166 | LE | TYPESET
MS Code : JTAC-D-18-02033 | CP | DISK

presence of at least two moisture fractions released below and above 100 °C, respectively. The occurrence of a high-temperature peak indeed is the fingerprint of the presence of gluten (Fig. 3) and can be an easy check of many "gluten-free" products [20]. However, the moisture fraction bound to gluten decreases when the dough is over-kneaded, namely when the gluten meshwork undergoes a mechanical stress, but comes back to the starting level after a two-hour rest [29]. If the overstressed dough immediately undergoes baking, it releases a larger amount of water and the final product is drier and crispier (e.g., biscuit) [30]. The underlying reason is that weak driving forces, like those experienced in kneading and extruding, can displace a large fraction of water linked to polymers, so allowing an easier realignment of polymer chains and the formation of more tight supramolecular clusters or networks.

Since the vapor phase is pure water, the equilibrium condition with a condensed aqueous phase implies the equivalence of the water chemical potential, μ_W:

$$\mu^*_{W,vap} = \mu^*_{W,liq} + RT_{vap}\ln(a_W)$$

that is

$$T_{vap} = \frac{\Delta_{vap}\mu^*(T)}{R\ln(a_W)}$$

where "*" and R stand for "pure water" and the gas constant, respectively. Reminding that $a_W \leq 1$ and $\Delta_{vap}\mu^*(T) < 0$ for $T > T^*_{vap}$ (i.e., 373.15 K), a lower a_W implies a higher T_{vap}, as $\ln(a_W)$ has a steeply decreasing trend. When the temperature of the system is not far from the relevant T_g, a real equilibrium is never reached. This means that the system can host regions with different water activity and different temperature of vaporization, T_{vap}. This conclusion is in line with the results of NMR relaxation experiments [9].

The crumb sealed in a plastic bag does not lose moisture, but undergoes staling that implies short-range displacements of water because of the formation of amylopectin and amylose crystal phases [31]. Similar changes occur in pasta and other starchy products [32].

As a result, water activity decreases in a staling crumb [28] even when any water loss is prevented and the product hardens since the relevant glass transition rises above room temperature because mostly the plasticizing water migrates into the polymer crystal zones. A 24-h stale crumb can release the moisture fraction fixed by gluten only when heated up to 175 °C (Fig. 4), while practically all the moisture bound to the other polymers leaves the crumb at temperatures below 100 °C [28].

Minor additions of extra ingredients produce substantial changes. For example, the addition of non-starch carbohydrates, like arabino-xylans, to the original wheat dough implies reduction of the gluten-bound moisture fraction and a final crumb with coarser alveolar structure and slower staling [24]. The addition of gluten-free flours (like soy, buckwheat, rice) delays the denaturation threshold of the globular proteins, whose exothermic effect can be "disentangled" from the endothermic one related to the starch gelatinization in DSC traces [20], and produces a denser loaf with smaller alveoli (although in a larger number per mL).

These pieces of information coupled with extra data, like elastic and rheological moduli [18], support some reliable conclusions about the macroscopic changes occurred in the system. NMR and X-ray diffraction provide evidence of changes at the molecular level either in the crust or in the crumb regions of the loaf [7, 9, 33–36].

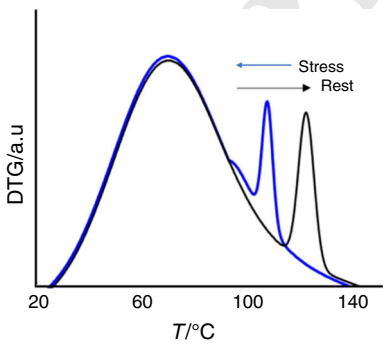

Fig. 3 DTG trace from a wheat flour dough. The high T peak concerns the moisture fraction bound to gluten. The temperature of this peak decreases when the dough undergoes a mechanical stress, like over kneading, but turns back to the original value after two-hour rest at room temperature

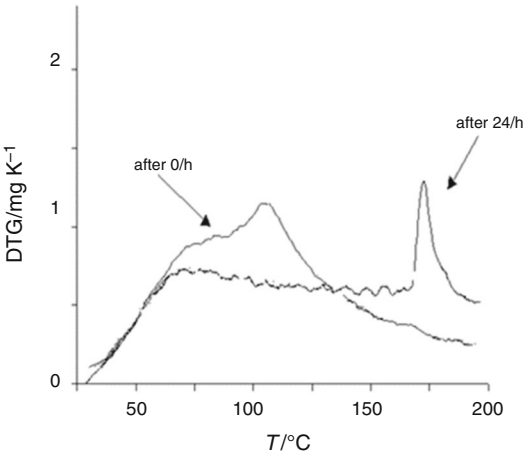

Fig. 4 DTG traces of stale crumb sealed in a plastic bag for 0 and 24h. Data from ref [28]

Journal : Large 10973 | Dispatch : 4-3-2019 | Pages : 12
Article No. : 8166 | LE | TYPESET
MS Code : JTAC-D-18-02033 | CP | DISK

Starch and other components

Much simpler is the study of the behavior of single ingredients of the dough, like an aqueous suspension of starch granules, requiring just standard DSC investigations to monitor the progress of the starch gelatinization in different conditions, namely water content, salt concentration, presence of proteins, or fats, etc. MTDSC [37] provides a better evidence especially when the investigation implies heating/cooling cycles (Fig. 5).

These studies show that the starting heterogeneity of the system (aqueous suspension of starch granules) becomes a mixed amylose/amylopectin gel that, when heated above 85 °C, becomes a sol system containing some amylose crystals and, in the presence of endogenous fats, amylose–lipid complexes. These complexes undergo fusion at about 110 °C, while the amylose crystals melt above 135 °C [38]. On cooling from 150 °C to room temperature, the amylose/lipid complexes undergo a partial restoration, and the final system is an amylopectin gel containing three types of crystals (amylose crystals, amylose/lipid complexes, amylopectin crystals) that show different X-ray diffraction patterns [7].

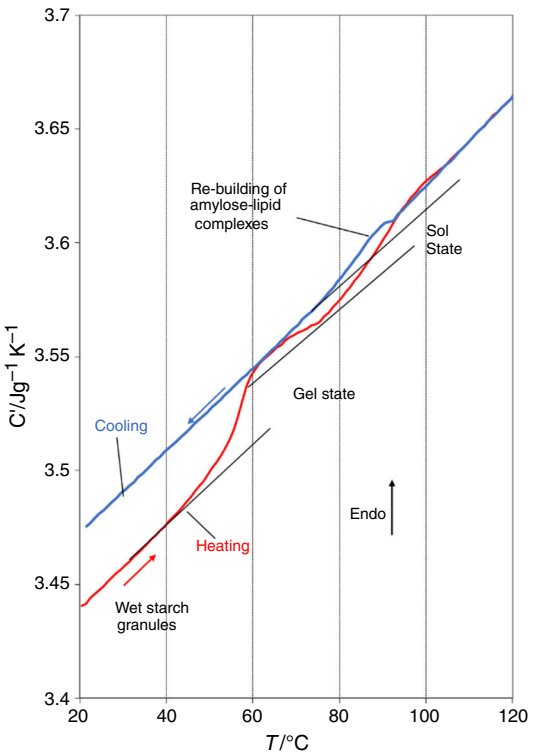

Fig. 5 Heating–cooling MTDSC traces of the in-phase heat capacity, C', of an aqueous suspension of wheat starch granules. The red trace is the first heating run, while the blue one corresponds to the cooling run. The evidence clearly shows the irreversibility of the starch gelatinization, while starch–lipid complexes (lipids are always associated with wheat starch granules) undergo fusion on heating and at least a partial reconstruction on cooling. Data from Ref. [38]

Specific investigations devoted to check the role or the effect of ionic strength, or simple sugars, on starch gelatinization, showing that cations and anions produce different effects [39] on starch gelatinization, while the addition of simple sugars normally delays the onset of the gelatinization and reduces its extent [40]. These results are relevant to nutritional issues, especially those related to diabetic consumers.

Non-aqueous food systems: the case of cocoa butter

Fats are the major family of non-aqueous food components (others are terpenes, hydrophobic vitamins, some aroma compounds, etc.). Many real food products can contain separate aqueous and fat layers or finely disperse phases (emulsions), or mechanically mixed ice and lipid crystals (ice cream), or mixtures of different lipids (edible oil, butter, margarine, etc.). The study of such systems once again requires the disentanglement of different processes that can occur simultaneously. The standard approach obviously is the investigation of single substances or mixtures of homologous compounds. An interesting system to study is cocoa butter, which indeed is a mixture of triacylglycerols (TAG) that behaves like a solid solution with its own polymorphic crystal phases. These show a monotropic behavior, namely each crystal phase has its own melting point and there are no transition temperatures between polymorphs. According to Wille and Lutton [41], there are six polymorphs with different melting points and fusion enthalpies (Table 1).

The DSC evidence is an endothermic signal that corresponds to the fusion of the crystals. In the case of cocoa-based products, a large number of DSC traces, collected to investigate the TAG polymorphous transitions in cocoa butter, cocoa liquor and dark chocolate, showed that these transitions have an extent and occur with a kinetics that largely depend on the previous thermal history [42]. The

Table 1 TAG polymorphs in cocoa butter according to [41]

Polymorph	T_{fus}/ °C	Δ_{fus} H/Jg^{-1}
I	17.3	Not appl.
II	23.5 ± 1.0	86.15
III	26.0 ± 0.5	112.47
IV	29.0 ± 0.5	117.47
V	31.3 ± 0.5	136.73
VI	36.0 ± 1.5	148.02

Journal : Large 10973 Dispatch : 4-3-2019 Pages : 12
Article No. : 8166 LE TYPESET
MS Code : JTAC-D-18-02033 CP DISK

contribution of the various polymorphs to the DSC endotherm of cocoa butter samples that had undergone a previous thermal history, namely annealing at various temperatures, comes out through a deconvolution treatment (Fig. 6).

The results are at the fundamental of a kinetic model [42] that describes the progress of the TAG evolution toward the most stable crystal form,

$$\text{Amorphous} \xrightarrow{k_1(T)} IV \xrightarrow{k_2(T)} V \xrightarrow{k_3(T)} VI$$

The kinetic model predicts the final crystal phases after any annealing history [42]: a result of obvious interest to explain the blooming of chocolate during the shelf life [43] and plan the industrial production process.

As mentioned, complementary information collected through other experimental approach can perfect the description of the system. Laser confocal microscopy and rheology investigations [44] demonstrated that TAG polymorphism reflects a hierarchical scale of structures at the mesoscopic level: Aggregates of small crystals form domains (spherulites) linked to one another in a fractal network that hosts a liquid (amorphous) phase within its meshes. The fractal dimension of the network would depend on the size of the spherulites, which in turn depends on the growth extent of the specific TAG polymorph(s), determined by the cooling rates and annealing temperatures. The final mesoscopic structure of the system (size of spherulites, fractal dimensions and fraction of amorphous/liquid phase) affects the rheological properties of the products.

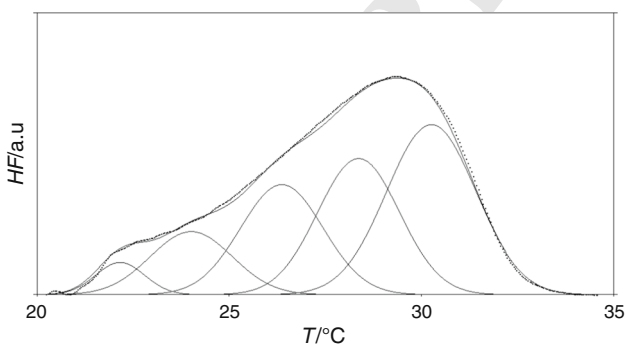

Fig. 6 Deconvolution of the endothermic DSC signal of the fusion of a cocoa butter sample. The Gaussian peaks correspond to the contributions of different TAG polymorphs (I, II, III, IV and V) present in the sample after a given annealing treatment. Not published data (experimental details in Ref. [42])

Shelf life and microbial spoilage

Another field of application of TAC in food science concerns the shelf life, during which food products undergo many changes of structure, texture, composition, etc., related to a number of factors, like formation of crystal phases, dehydration, oxidation, microbial spoilage.

Structural and composition changes

Food products undergo physical changes, as they are metastable systems tending to attain more or less slowly some equilibrium state. This is typical of dispersed systems [45]. Foams, emulsions and suspensions tend to collapse and separate in bulk phases. Amorphous solids tend to crystallize whenever the local molecular mobility is large enough to allow short-range displacements. Water migrates along local gradients of chemical potential across phase boundaries and/or escape toward the head–space of the system. These changes produce substantial modifications of texture, color, taste and flavor and often make the product unacceptable by the consumer. A good example comes again from starchy products that undergo staling [16, 18]. TAC experiments allow a quantitative assessment of this change and its progress on ageing (see above).

The most important composition change that affects the properties of food is the decrease in the moisture content. The change is often desired as drying is an old practice to preserve food.

Besides thermal and freeze-dry dehydration, osmo-dehydration is a mild treatment that does not severely affect the original properties of the starting product, as in the case of fruits and vegetables whose moisture content can account for more than 85% of the overall mass. The process requires the use of a hypertonic medium where to pour the food. The consequent displacement of water affects both the extra- and the intracellular regions. Actually, a gradient of water activity between the hypertonic medium and the extracellular region drives water toward the former (whose composition remains practically unaffected because of its overwhelming mass). Since there is no semipermeable barrier between these fluids, some solute (e.g., sugar) of the hypertonic medium enters the extracellular region and remains there at the end of the process. The intracellular water trespasses the cell membranes toward the extracellular region. Because of this moisture depletion, the fruit shrinks keeping its basic structure, which can turn back to the starting status almost completely on rehydration, save for the trapped sugar. Knudsen TG is a suitable tool to monitor the process and provides data that allow description of all its steps, including the shrinkage [14]. The corresponding DTG trace reflects the flux, J_W, of

Journal : Large 10973 Dispatch : 4-3-2019 Pages : 12
Article No. : 8166 LE TYPESET
MS Code : JTAC-D-18-02033 CP DISK

escaping water that depends on the gradient of the chemical potential, $\nabla\mu_W$,

$$J_W = \frac{1}{A}\frac{dm}{dt} = \frac{DTG}{A} \propto -D_W \nabla \mu_W$$

where A and D_W stand for cross-sectional area and diffusion coefficient, respectively. The dehydration of a sample in Knudsen regime implies the simultaneous detection of water activity and water content, which therefore allows the direct assessment of the dehydration isotherm [26]. If one performs the Knudsen dehydration of partially osmo-dehydrated samples, he can accordingly define both the dry mass and the water activity at every intermediate step of the process. It comes out that the desorption trend of the osmo-dehydrated food tends to overlap that of the hypertonic medium (Fig. 7) for large drying extents [14].

This reflects the decrease in the overall mass of the intracellular region. Since the three fluids (hypertonic medium, extra- and intracellular regions) must have the same water activity at any step of the process, the gap between the desorption trends of non-treated sample and hypertonic medium can be used to predict the mass proportion between intra- and extracellular regions in a partially osmo-dehydrated sample applying the classic lever rule [14]. This finally leads to a likely estimation of the shrinkage of the sample, assuming that the volume of the moisture lost is the main contribution [14] to the process.

Oxidation

Another crucial issue related to the shelf life of most food products is oxidation. The addition of antioxidants, vacuum-sealing or inert atmosphere can delay the process. Some food products are naturally rich of antioxidant compounds and therefore are easier to preserve. However, because of the multi-component and multi-phase nature of most food, a quantitative assessment of the antioxidant potential of a given product is not easily achievable. In most cases, such evaluation comes from experimental data drawn with independent methods, most of which require preliminary time-consuming treatments.

Reaction calorimetry (RC) allows determination of the exothermic effect related to the scavenging of oxygen or oxidants, regardless of the physical form of the sample and without the need of sample pretreatments. RC can therefore be of help to describe the behavior of the antioxidant potential of many food systems [46].

A common natural antioxidant is ascorbic acid (AA). When matched with H_2O_2, AA (one should better say ascorbate anion) produces a large exothermic effect that, for small AA concentrations ([AA] $\leq$ 500 mM), appears as a single peak in the isothermal RC trace. Nonetheless, at larger concentrations, the signal shows a shoulder that suggests an underlying multi-step reaction mechanism. It is known that the oxidation of AA occurs via radical intermediates with the formation of dehydroascorbic Acid (DHA), diketogulonic acid (DKGA) and the end product 4,5,5,6-tetra hydroxyl-2,3-di-keto-hexanoic acid (THDHA). Each step would imply its own thermal effect that contributes to the overall signal detected. For the sake of simplicity, a simpler scheme of two consecutive steps involving the known intermediate compounds may be of help to suggest an interpretation of the signal (Scheme 2).

This scheme implies a simple solution and a correspondent expression for the related heat flow:

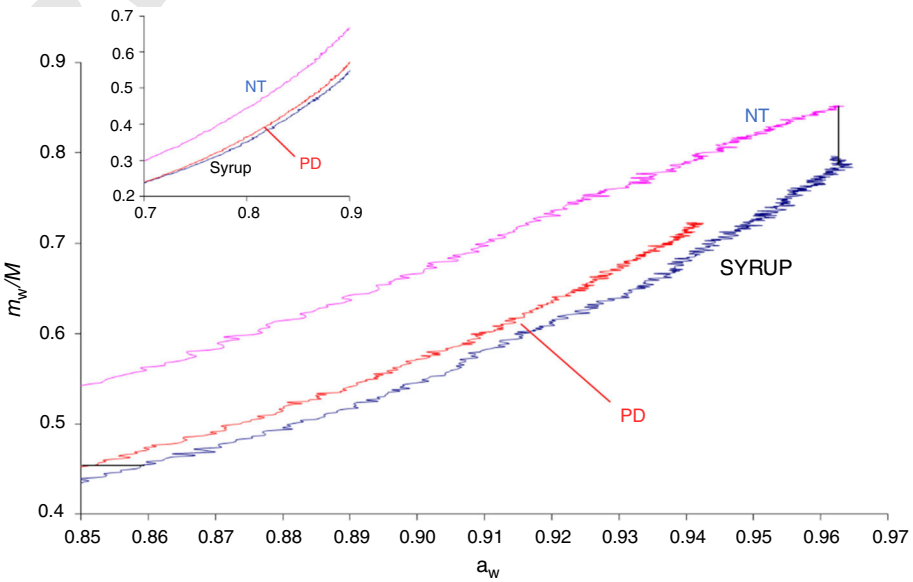

Fig. 7 Knudsen desorption isotherms of non-treated (NT) and partially osmo-dehydrated apple pulp (PD), compared with that of the hypertonic syrup used for the osmo-dehydration. The inset shows that the desorption trend of PD tends to overlap the one of SYRUP for large dehydration extents. Adapted from Ref. [14])

Journal : Large 10973 Dispatch : 4-3-2019 Pages : 12
Article No. : 8166 LE TYPESET
MS Code : JTAC-D-18-02033 CP DISK

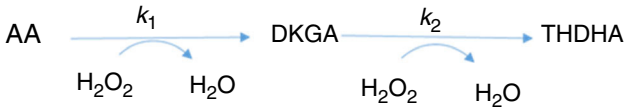

Scheme 2 Simplified reaction steps of the oxidation of AA with hydrogen peroxide [46]

$$\dot{Q} = \left[k_1\Delta H_1 + \frac{k_1k_2}{k_2 - k_1}\Delta H_2\right]e^{-k_1t} - \left[\frac{k_1k_2}{k_2 - k_1}\Delta H_2\right]e^{-k_2t} = ae^{-ct} - be^{-dt}$$

The best fit of the RC trace leads to recognize that $\Delta H_1 < 0$ and $\Delta H_2 > 0$. Accordingly, one can split the overall signal in two contributions,

$$k_1\Delta H_1 e^{-k_1t} = \mathrm{d}Q_1/\mathrm{d}t$$

$$\frac{k_1k_2}{k_2 - k_1}\Delta H_2\left[e^{-k_1t} - e^{-k_2t}\right] = \mathrm{d}Q_2/\mathrm{d}t.$$

Figure 8 reports an example of such split.

Having so defined the oxidation process of AA, one can determine the antioxidant power of a given food product (usually wine, fruit juices or liquid products) versus hydrogen peroxide matching the heat released with that obtained with known amounts of ascorbic acid (AA) at given pH and temperature conditions. This procedure allows the assessment of a rank of antioxidant capacity of various food products, expressed as ascorbic acid equivalents [46]. Similar investigations concern spent coffee [47], tocopherols [48] and linoleic acid [49].

Microbial spoilage

The most important changes during the shelf life depend on the microbial spoilage, which takes place when the relative humidity (RH) is larger than 70% (lower thresholds apply for molds and enzymatic processes) [50, 51]. This is why the control of RH is compulsory for food technologists.

Isothermal calorimetry (IC) is an ideal tool to monitor the presence and the growth of microbial organisms, no matter whether single or many microbial strains are present, in almost any kind of medium and represents a valid alternative to the plate counts, not requiring any preliminary treatment [52].

The increase in the microbial population is the neat balance between growth (exothermic) and death (normally endothermic) of cells, although the former implies a much larger thermal effect. Beside the neat exothermic balance related to the growth progress, one should account for the fact that, in a microbial culture, some aged cells do not duplicate, but still are able to uptake and metabolize the available substrate, which implies an extra neat exothermic effect proportional to the number of viable cells [53]. Therefore, the observed thermal effect, $\dot{Q}$, appears as a large exothermic signal that reflects the growth progress and the non-growth cell metabolism, namely

$$\dot{Q} = \dot{N}q_g + N\dot{q}_m$$

where q_g and $\dot{q}_m$ are the heat released by a single duplicating cell and the metabolic non-growth heat flow of a single viable cell, respectively, while N and $\dot{N}$ stand for number of viable cells and growth rate. However, the calorimetric signal appears only when $\dot{Q}$ is significantly larger than the detectability threshold of the instrument used, namely 0.1 μW/mL for standard calorimeters [54]. This implies that the onset of the calorimetric signal occurs substantially later than the onset of the growth trend and corresponds to the attainment of the detectability threshold of the instrument (Fig. 9).

During the span between growth and signal onsets, both the microbial population within the calorimetric cell and

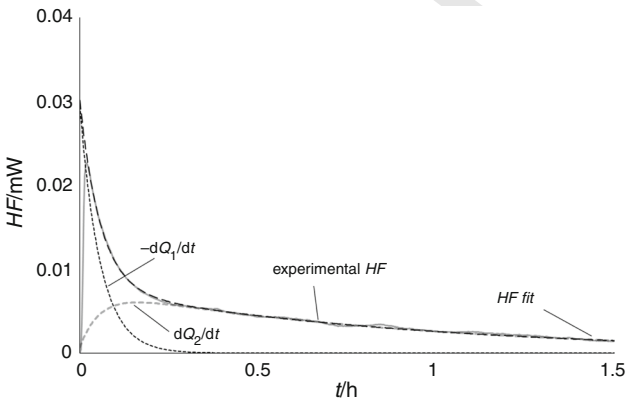

Fig. 8 Split of the RC isothermal trace of AA oxidation with excess H_2O_2 in the sum of an exo- and an endothermic contribution. [AA] = 0.25 mM. Not published data (experimental details in Ref. [46])

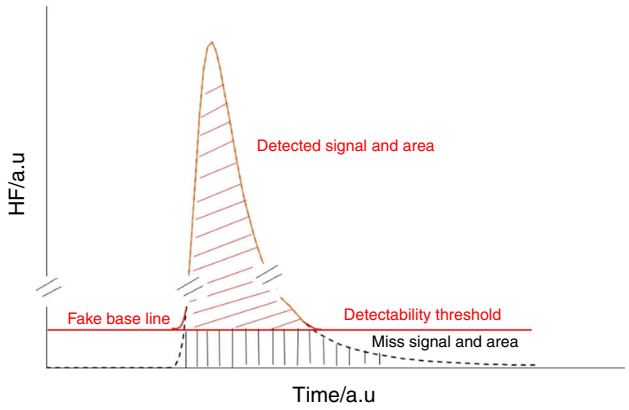

Fig. 9 The onset of the calorimetric trace can appear rather smooth and broad: this shape has nothing to do with the actual trend of the growth, but simply reflects the trespass through the detectability threshold

Journal : Large 10973 Dispatch : 4-3-2019 Pages : 12
Article No. : 8166 LE TYPESET
MS Code : JTAC-D-18-02033 CP DISK

the growth rate increase by some orders of magnitude. When the microbial population approaches its end steady level, the growth rate vanishes. The relevant thermal effect can again drop below the detectability threshold, unless the metabolic contribution $N\dot{q}_m$ is sufficiently large because of the high value attained by N. In other words, IC only partially "perceives" the growth progress at its beginning and at its end. The so-called lag phase that usually precedes the growth onset is expected to imply a very low heat flux (less than 0.1 fW/CFU), therefore remaining hardly detectable even with very sensitive instruments.

A critical issue to consider is that microbial growth in food systems is not the same as in planktonic conditions, *i.e.*, cells dispersed in an aqueous solution of nutrients. In real systems, the progress of the microbial growth can substantially modify the surrounding environment implying change of pH, ionic strength, substrate concentration [55] and, of course, the available volume to accommodate the new cell generations.

To achieve a reliable view of what is happening in a real system, one needs to perform separate experiments with a single microbial species in planktonic conditions and check the changes produced by varying the medium pH, the temperature and, tentatively, by adding some extra microbial species or adverse compounds [56]. Of great help are extra data, possibly collected from the same system that is undergoing the calorimetric investigation (Fig. 10). This implies the use of special calorimetric cells that allow the insertion of extra sensors to detect pH, color changes, or the concentration of given probe compound [55].

Finally, one has to translate all these pieces of information in a clear picture of the microbial growth that may occur in a real system. For example, one may attempt an interpretation of the experimental overall evidence through models of microbial growth [57, 58]. However, the assessment of N and $\dot{N}$ is unachievable through an "a priori" approach, as the number of variables involved in real systems is large and can differ from case to case [59, 60]. An interpretation of the calorimetric signal (and experimental evidences of the traditional microbiology investigations) that does not require the use of a growth model is therefore of great interest.

A semiempirical approach, based on some experimental evidence, like plate counts, has proven rather adequate whenever the microbial strain grows via duplication mechanism [61, 62], namely $N = N_0\, 2^{t/\tau(t)}$, where N_0 and τ (t) are the starting microbial population and the generation time, respectively (Fig. 11).

It is important to notice that the plate count data are commonly reported in a semilogarithmic scale, the slope of which corresponds to the so-called specific growth rate, $\dot{N}/N$, while the calorimetric signal is related to the absolute growth rate, $\dot{N}$, which shows a maximum quite later than the former, and to N.

In the considered example, N_0 is close to 10^2 CFU, while the end steady values of N are about 10^9 CFU. This means that the end tail of the IC trace would reflect the microbial non-growth metabolism if $\dot{q}_m$ is larger than 0.1 fW/CFU.

The proposed semiempirical model suggests the following fitting expression for the IC trace:

$$\dot{Q} = q_g\left[N_0 \times 2^{t/\tau} \times \log_e(2) \times \frac{\tau - t\dot{\tau}}{\tau^2}\right] + \dot{q}_m\left[N_0 \times 2^{t/\tau}\right]$$

where $\tau = \left(\frac{a}{t} + bt\right)$ is the generation time [61, 62]. To account for the delayed onset of the IC signal, one has to replace t with $(t - \Delta t)$ in every expression used. This is tantamount as to replace the microbial culture with a virtual one with the same starting N_0, and a generation time

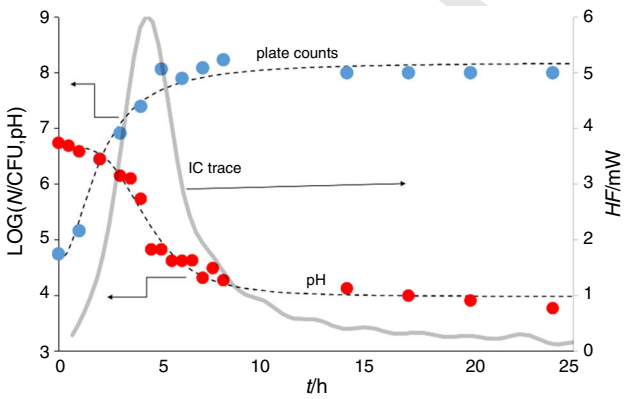

Fig. 10 Streptococcus thermophilus. IC trace, plate counts and pH Adapted from ref [55]: fitting dotted lines for plate counts and pH according to the semiempirical model (see text below) and dose-logistic model, respectively

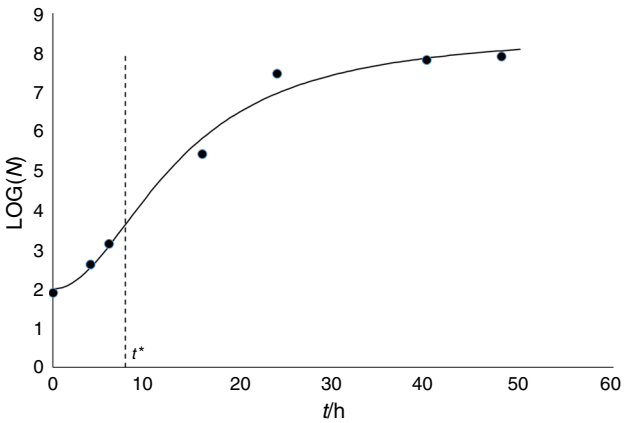

Fig. 11 An application of the proposed empirical model to fit the experimental plate counts of *L. helveticus*. The maximum of the specific growth rate ($\dot{N}/N$) occurs at $t = t^*$, when the growth progress reaches ¼ of the overall growth span in logarithmic scale [61]

Journal : Large 10973 Dispatch : 4-3-2019 Pages : 12
Article No. : 8166 LE TYPESET
MS Code : JTAC-D-18-02033 CP DISK

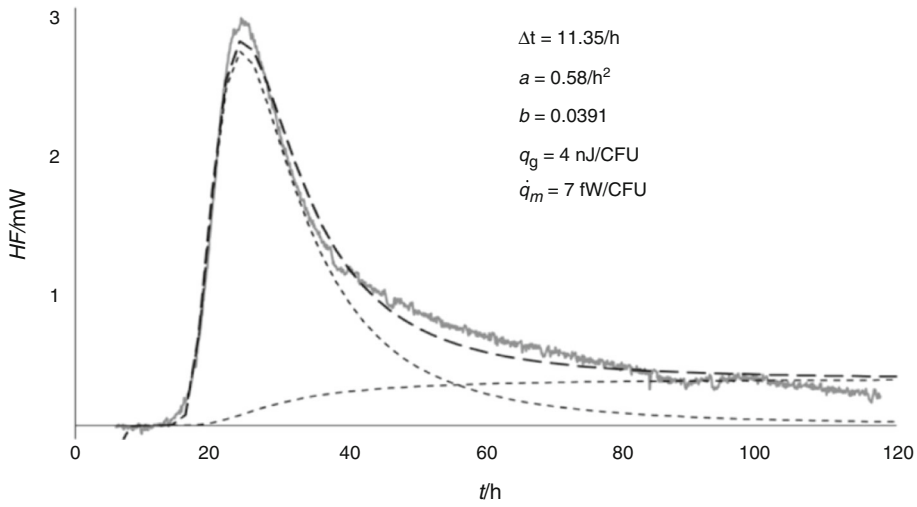

Fig. 12 IC trace of a culture of *L. helveticus* (10^3 CFU in 6 mL, at 37 °C). The heavy dashed line corresponds to the fit obtained with the proposed semiempirical model (see text) that allows the splitting of the signal in growth and non-growth contributions (dotted lines). The inset reports the best-fitting parameters

that is a little larger in the early phase of the growth (that anyway escaped from the IC detection) but becomes a little smaller during the so-called exponential growth phase. The parameters Δt, a, b, q_g and $\dot{q}_m$ come from the fitting routine. Figure 12 shows the result.

The reliability of the q_g and $\dot{q}_m$ values is obviously limited to the respective order of magnitude as they come from the product between very large (N or $\dot{N}$) and very small (q_g or $\dot{q}_m$) quantities. Nonetheless, they can be of some interest for those who are involved in the study of cell biochemistry. These values of q_g and $\dot{q}_m$ allow estimation of the threshold IC detectable levels of N and $\dot{N}$, namely 10^6 CFU/mL and 5 CFU mL^{-1} s^{-1}, respectively.

A threshold value of 10^6 CFU/mL may seem rather high, casting some doubts about the practical use of calorimetry to monitor microbial growth. However, it is not so when considered in the appropriate perspective: Namely, real situations imply population densities of this (or higher) order of magnitude that are too large for the standard practice of the microbiological plate counts. Plate counts indeed require a previous dilution of the sample, which implies loss of accuracy. The calorimetric approach does not require a previous dilution of the original sample that can directly undergo the calorimetric investigation without any preliminary preparation.

Conclusions

Some examples of TAC investigations applied to food products or their ingredients show that these experimental approaches, combined with side information from other techniques, allow one to shed light on the properties of these multi-phase and multi-component systems. However, the investigator needs to put at work a specific expertise to select the suitable instrument and envisage an adequate experimental plan, according to the available tools.

A special attention requires the interpretation of the collected data, as food systems undergo simultaneous and concurrent changes that produce an overall instrumental output, which may appear neat and simple, but actually is the resultant of many contributions.

The need of separate investigations dealing with simple model systems is a way to disentangle different transformations that occur in the same temperature range or time span. Mathematical deconvolution of the recorded signals is a major tool to use, but the underlying physical models require a critical scrutiny to avoid oversimplifications or imply unsuitable assumptions.

Kinetic models can usually be of help, because of the intrinsically dynamic nature of the system under study, as in the case of microbial cultures. However, semiempirical approaches seem more reliable than a priori schemes, since, although not providing general "laws", they can account for the peculiarities of the system under study through adjustable fitting parameters, whose physical meaning may appear a posteriori [61, 62].

References

1. Schiraldi A, Lilley TH, Braibanti A, Ollivon M, Cesaro A, Masi P. Calorimetry, thermal analysis and chemical thermodynamics in food science: Report on the panel discussion. Thermochim Acta. 1990;162:253–64.
2. Applications of calorimetry and thermal-analysis to food systems and processes. Thermochim Acta, 246 (1994) Special Issue, R11-R12, guest Ed. A. Schiraldi.
3. Schiraldi A, Piazza L, Fessas D, Riva M, in Handbook of thermal analysis and calorimetry (1999) chap. 16, R. Kemp Ed., Elsevier Publ., Amsterdam, 829–921.

Journal : Large 10973 | Dispatch : 4-3-2019 | Pages : 12
Article No. : 8166 | LE | TYPESET
MS Code : JTAC-D-18-02033 | CP | DISK

4. Slade L, Levine H. Beyond water activity: recent advances based on an alternative approach to the assessment of food quality and safety. Critical Rev Food Sci Nutr. 1991;30:115–360.
5. Tolstoguzov VB. Some thermodynamic considerations in food formulation. Food Hydrocolloids. 2003;17:1–23.
6. Bubbles in food, (1999), G.M. Campbell, C. Webb, S.S. Pandiella and K. Nirajan, Eds., Eagan Press Publ.
7. Schiraldi A, Fessas D, Signorelli M. Water activity in biological systems-a review. Pol J Food Nutr Sci. 2012;62:5–13.
8. Zobel HF. Starch crystal transformations and their industrial importance. Starch. 1988;40:1–7.
9. Hills BP Water management in the design and distribution of quality foods", (1999) Y.H. Roos, R.B. Leslie and P.J. Lillford Eds., Technomic Publ. Co., Lancaster, Penn., USA, 107-131.
10. Beltonen PS. J Cereal Sci. 1999;29:103–7.
11. Schiraldi A, Piazza L, Riva M. Bread staling: a calorimetric approach. Cereal Chem. 1996;73:32–9.
12. Schiraldi A, Fessas D, Signorelli M, in "Calorimetry in food processing", G. Kalentuc Ed., IFT Press series (2009), chap 11.
13. Krokida MK, Karathanos VT, Maroulis ZB. Effect of freeze-drying conditions on shrinkage and porosity of dehydrated agricultural products. J Food Eng. 1998;35:369–80.
14. Lewicki PP. Design of hot air drying for better foods. Trends Food Sci Technol. 2006;17:153–63.
15. Pani P, Schiraldi A, Signorelli M, Fessas D. Thermodynamic approach to osmo-dehydration. Food Biophys. 2010;5:177–85.
16. Roos HY. Water activity and physical state effects on amorphous food stability. J Food Process Preserv. 1993;16:433–47.
17. Roos HY. Phase transitions in foods. San Diego: Acad. Press Inc.; 1995.
18. H. This, "Molecular Gastronomy: exploring the science of flavors" (2005), ISBN: 023114170X.
19. Larsson H, Eliasson A-C. Cereal Chem. 1996;73:18–31.
20. Fessas D, Signorelli M, Pagani A, Mariotti M, Iametti S, Schiraldi A. Guidelines for buckwheat enriched bread: thermal analysis approach. J Therm Anal Cal. 2008;91:9–16.
21. Tolstoguzov VB. Foods as dispersed systems. Thermodynamic aspects of composition-property relationships in formulated food. J Therm Anal Cal. 2000;61:397–409.
22. Piazza L, Masi P. Moisture redistribution throughout the bread loaf during staling and its effects on mechanical properties. Cereal Chem. 1995;72:320–5.
23. Mitchell JR, Fan JT, Blanshard JMV. Bubbles in food (1999), G.M. Campbell, C. Webb, S.S. Pandiella and K. Nirajan, Eds., Eagan Press Publ.
24. Fessas D, Schiraldi A. Texture and staling of wheat bread crumb: effects of water extractable proteins andpentosans'. Thermochim Acta. 1998;323:17–26.
25. Fessas D, Schiraldi A. Starch Gelatinization Kinetics in Bread Dough. DSC investigations on'simulated'baking processes. J Therm Anal Cal. 2000;61:411–23.
26. Schiraldi A, Fessas D. Classical and Knudsen thermogravimetry to check states and displacements of water in food systems. J Therm Anal Cal. 2003;71:221–31.
27. Schiraldi A, Piazza L, Brenna O, Vittadini E. Structure and properties of bread dough and crumb. J Therm Anal. 1996;47:1339–60.
28. Fessas D, Schiraldi A. Water properties in wheat flour dough II: classical and Knudsen thermogravimetry approach. Food Chem. 2005;90:61–8.
29. Fessas D, Schiraldi A. Water properties in wheat flour dough I: classical thermogravimetry approach. Food Chem. 2001;72:237–44.
30. Piazza L, Schiraldi A. Correlation between fracture of semi-sweet hard biscuits and dough viscoelastic properties. J Texture Stud. 1997;28:523–41.
31. Schiraldi A, Fessas D. Bread staling (2000), P. Chinachoti, Y. Vodovotz, Eds., CRC, Boca Raton, FL, 1–17.
32. Riva M, Fessas D, Schiraldi A. Starch retrogradation in cooked pasta and rice. Cereal Chem. 2000;77:433–8.
33. Kou Y, Ross EW, Taub LA. Amorphous food and pharmaceutical systems, (2002) H. Levine Ed., The Royal Society of Chemistry, Cambridge, 48–58.
34. Hall L-D, Amin MHH, Evans S, Nott KP, Sun L. Water science for food, health, agriculture and environment, Z. Berk, R.B. Leslie, P.J. Lillford and S. Mizrahi Eds., Technomic Publ., Lancaster, Penn., USA, 255–271.
35. Schiraldi A. Starch and starch containing products: origins - structure, properties and new technologies", V. Yuryev, A. Cesaro and W. Bergthaller Eds., Nova Science Publishers, (2002) chap 20, 287–296.
36. Vodovotz Y, Vittadini E, Sachleben JR. Use of 1H cross-relaxation nuclear magnetic resonance spectroscopy to probe the changes in bread and its components during aging. Carbohydr Res. 2002;337:147–53.
37. Schiraldi A, Fessas D, Signorelli M, data presented at ESTAC 9, Kracow, August 27–31, 2006.
38. Yuryev VP, Krivandin AV, Kiseleva VI, Wasserman LA, Genkina NK, Fornal J, Błaszczak W, Schiraldi A. Structural parameters of amylopectin clusters and semi-crystalline growth rings in wheat starches with different amylose content. Carbohydr Res. 2004;339:2683–91.
39. Lii CY, Lee BL. Cereal Chem. 1993;70:188–92.
40. Hedayati S, Shahidi F, Koocheki A, Farahnaky A, Majzoobi M. Physical properties of pregelatinized and granular cold water swelling maize starches at different pH values. Int J Biol Mol. 2016;88:499–504.
41. Wille RL, Lutton ES. Polymorphism of cocoa butter. J Am Oil Chem Soc. 1966;43:491–6.
42. Fessas D, Signorelli M, Schiraldi A. Polymorphous transitions in cocoa butter: a quantitative DSC study. J Therm Anal Cal. 2005;82:691–702.
43. Aguilera JM, Michel M, Mayor G. Fat migration in chocolate: diffusion or capillary flow in a particulate solid?—a hypothesis paper. J Food Sci. 2004;69:167–74.
44. Narine SS, Marangoni AG. Relating structure of fat crystal networks to mechanical properties: a review. Food Res Int. 1999;32:227.
45. Tolstoguzov VB. Texturising by phase separation. Biotechnol Adv. 2006;24:626–8.
46. Kamrul HSM, Schiraldi A, Cosio MS, Scampicchio M. Food and ascorbic scavengers of hydrogen peroxide. J Therm Anal Cal. 2016;125:729–37.
47. Haman N, Ferrentino G, Imperiale S, Scampicchio M. Antioxidant and prooxidant activity of spent coffee extracts by isothermal calorimetry. J Therm Anal Cal. 2018;132:1065–75.
48. Haman N, Longo E, Schiraldi A, Scampicchio M. Radical scavenging activity of lipophilic antioxidants and extra-virgin olive oil by isothermal calorimetry. Thermochim Acta. 2017;658:1–6.
49. Haman N, Romano A, Asaduzzaman M, Ferrentino G, Biasioli F, Scampicchio M. A microcalorimetry study on the oxidation of linoleic acid and the control of rancidity. Talanta. 2017;164:407–12.
50. Labuza TP, McNally L, Gallagher D, Hawkes J, Hurtado F. Stability of intermediate moisture foods. 1. Lipid oxidation. J Food Sci. 1972;37:154–9.
51. Rahman MS, Labuza TP. Water activity and food preservation, Handbook of Food Preservation, 2nd ed. (2007) M.S. Rahman, Ed., CRC Press, Boca Raton, Florida, USA, 447-476.

Journal : Large 10973 | Dispatch : 4-3-2019 | Pages : 12
Article No. : 8166 | ☐ LE | ☐ TYPESET
MS Code : JTAC-D-18-02033 | ☑ CP | ☑ DISK

52. Schiraldi A. The nature of biological systems as revealed thermal methods"(2004) chap.2, D. Lorinczy Ed., Kluwer Academy Publ., 31.
53. Schiraldi A. Microbial growth and metabolism: modelling and calorimetric characterization. Pure Appl Chem. 1995;67:1873–8.
54. Fessas D, Schiraldi A. Isothermal calorimetry and microbial growth: beyond modeling. J Therm Anal Calorim. 2017;130:567–72.
55. Riva M, Fessas D, Franzetti L, Schiraldi A. Calorimetric characterization of different yeast strains in doughs. J Therm Anal Calorim. 1998;52:753–64.
56. Gardikis K, Signorelli M, Ferrario C, Schiraldi A, Fortina MG, Hatziantoniou S, Demetzos C, Fessas D. Microbial biosensors to monitor the encapsulation effectiveness of Doxorubicin in chimeric advanced drug delivery nano systems: a calorimetric approach. Int J Pharm. 2017;516:178–84.
57. Baranyi J, Pin C, Ross T. Validating and comparing predictive models. Int J Food Microbiol. 1999;48:159–66.
58. Buchanan RL, Whiting RC, Damert WC. When is simple good enough: a comparison of the Gompertz, Baranyi, and three-phase linear models for fitting bacterial growth curves. Food Microbiol. 1997;14:313–26.
59. Peleg M. Advanced quantitative microbiology for food and biosystems: models for predicting growth and inactivation. Boca Raton: CRC Press; 2006.
60. Peleg M. Microbial survival curves: interpretation, mathematical modeling and utilization. Comments Theor Biol. 2003;8(2003):357–87.
61. Schiraldi A. Cell Dev Biol 6 (2017) 185, https://doi.org/10.4172/2168-9296.1000185, and related appendix.
62. Schiraldi A. Single Cell Biol. 2017;6:166. https://doi.org/10.4172/2168-9431.1000166.
63. Schiraldi A. Data presented at MEDICTA 2017, Sept 24–27, Loano (Italy).
64. Fessas D, Schiraldi A. Isothermal calorimetry and microbial growth: beyond modeling. J Therm Anal Cal. 2017;130:567–72.

Journal : Large 10973 | Dispatch : 4-3-2019 | Pages : 12
Article No. : 8166 | ☐ LE | ☐ TYPESET
MS Code : JTAC-D-18-02033 | ☑ CP | ☑ DISK